

# Computer Simulation of Power Factor Corrected Circuits\*

R. GARCÍA-GIL, J. M ESPÍ AND J. CASTELLÓ

L.E.I.I, Dpto. Ingeniería Electrónica, University of Valencia, 46100 Burjassot, Spain.

E-mail: garciagi@uv.es

*An efficient method for simulating three-phase power factor corrected (PFC) converters, using MATLAB/SIMULINK<sup>®</sup>, is applied for the education and training of undergraduate students in power electronics. This simulation method requires a previous mathematical analysis of the proposed converter to obtain the SIMULINK commutation model, which allows students to acquire a better knowledge of the circuit. Two PFC rectifiers, i.e. voltage source (VSR) and current source (CSR) rectifiers, are analysed and simulated. Two different PFC controllers are considered: a sinusoidal-PWM (SPWM) controller for the VSR and the space vector modulation (SVM) technique for the CSR. With these SIMULINK models, students can carry design the controller and validate whether or not their closed loop system meets the prescribed performance requirements.*

**Keywords:** electrical engineering education; space vector modulation; power factor correction; voltage source rectifier; current source converters

## INTRODUCTION

DIGITAL CONTROL is being incorporated into power conversion thanks to the improvement in performance and fall in cost of digital-signal processors (DSPs) and microcontrollers [1]. This permits implementation of more sophisticated control techniques such as space vector modulation (SVM) for power factor corrected (PFC) circuits [2] and other modern control techniques (predictive control, optimal control, neuro-fuzzy control) for output regulation. In particular, the concept of SVM is quite difficult for the student to understand, since this calculus is considered to be an academic concept with limited practical application. In order to introduce these new subjects into a course of electrical engineering in an easy and attractive form, powerful simulation software tools that combine analogue and digital calculations are required.

Traditionally, the SPICE package [3] has been used to simulate the behaviour of power electronic converters in most courses, but its digital control features are limited and difficult to implement, introducing high calculation effort and convergence problems [4]. A new class of circuit simulators such as SIMPLORER [5] and PSIM [6] are equally conversant in digital control and circuit response, while having a low execution time with less numerical convergence problems, and are user-friendly. Nevertheless, MATLAB/SIMULINK<sup>®</sup> [7–9] is the most widely used mathematical tool for control design, modelling and simulation of

dynamic systems. It has, in reality, become a de facto standard.

The procedure used in this course for simulating power factor corrected (PFC) rectifiers uses SIMULINK. It consists of obtaining the state-space equations describing inductor currents and capacitor voltages. The discrete switching functions are also incorporated into the modelling equations to obtain details of the switching ripple. For the modelling of the power converter, ideal switches will be considered. All this analysis enables the student to gain a better understanding of the circuit and allows models for the design of the controllers to be obtained. Simulation is very useful, but it needs to be preceded by a previous circuit analysis. The extensive usage of circuit simulation packages leads to a loss of ability to perform the mathematical analysis of more complex circuits.

In this work we present the modelling of the two basic three-phase rectifiers: the voltage source rectifier (VSR) and the current source rectifier (CSR). For the VSR, a predictive controller [10] will be applied for power factor correction. For the CSR a space vector modulation (SVM) technique will be considered and different output profiles will be analysed, studying what configuration reduces the pollution that we introduce into the mains (limited by the new standards such as IEC 1000-3-2). The simulations performed with MATLAB/SIMULINK for these topologies have given a short simulation time with no convergence problems. Although previous results [4] have already discussed the use of SIMULINK for the simulation of three-phase rectifiers, none of them deals with the simulation of the SVM procedure.

\* Accepted 12 September 2006.

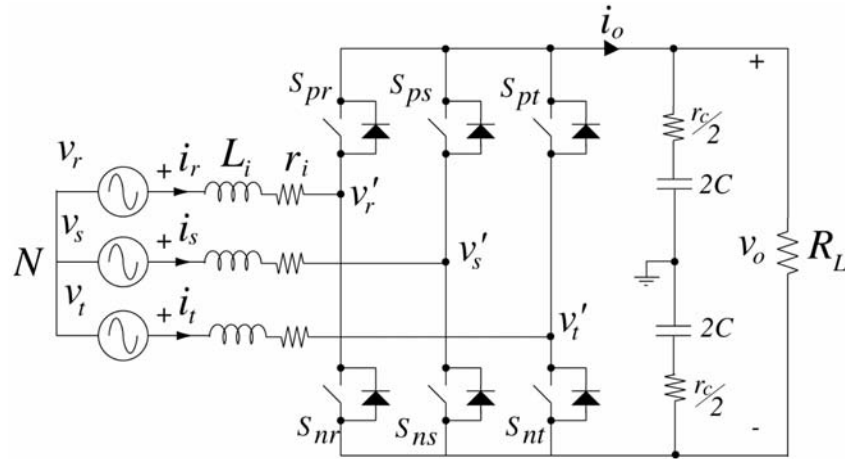


Fig. 1. Three-phase voltage source rectifier.

### MODELLING OF THE VSR

The voltage source rectifier (VSR) or three-phase boost rectifier (Fig. 1) is the most widely used rectifier for medium and high-power applications [11]. The main features are constant DC-link voltage ( $v_o$ ), low harmonic distortion of the mains currents with controllable power factor, and bidirectional current flow. In order to obtain sinusoidal current waveforms on the AC side, the six transistors can be controlled in a sinusoidal PWM (SPWM) manner [12].

For modelling consideration, the VSR can be divided into three parts: the line filter, the rectifier bridge with six current-bidirectional switches and the DC-link voltage with a resistive load ( $R_L$ ). The line filter and the DC-link are modelled by their corresponding state-space equations.

By applying Kirchoff's laws, the differential equations describing the input filter are

$$\dot{i}_j = -\frac{r_i}{L_i} + \frac{1}{L_i} \cdot (v_j - v'_j) \quad j = [r, s, t] \quad (1)$$

where the neutral point of the DC-link is referred to as the ground, in order to simplify the equivalent circuit modelling.

The state-space equations describing this block are

$$\begin{aligned} \dot{x} &= A_1 x + B_1 u \\ y &= C_1 x + D_1 u \end{aligned} \quad (2)$$

where  $x = [i_r \ i_s \ i_t]^T$ ,  $u = [v_r - v'_r \ v_s - v'_s \ v_t - v'_t]^T$  and  $y = x$  are the state, the input and the output vectors respectively. The obtained matrices  $A_1$ ,  $B_1$ ,  $C_1$  and  $D_1$  are

$$\begin{aligned} A_1 &= \frac{-r_i}{L_i} \text{eye}(3); & B_1 &= \frac{1}{L_i} \text{eye}(3); \\ C_1 &= \text{eye}(3); & D_1 &= \text{zeros}(3, 3) \end{aligned} \quad (3)$$

To avoid line inductor open-circuit and DC-link capacitor short circuit, the two switches of each rectifier leg must be complementary, so the switching functions for the VSR can be defined as

$$S_j = \begin{cases} 1 & S_{pj} \text{ ON, } S_{nj} \text{ OFF} \\ -1 & S_{pj} \text{ OFF, } S_{nj} \text{ ON} \end{cases} \quad j = [r, s, t] \quad (4)$$

The voltages at the rectifier input ( $v'_r, v'_s, v'_t$ ) and the output current ( $i_o$ ) are

$$\begin{aligned} v'_j &= \frac{v_o}{2} \cdot S_j \quad j = [r, s, t] \\ i_o &= \frac{1}{2} \cdot (S_r i_r + S_s i_s + S_t i_t) \end{aligned} \quad (5)$$

Concerning the DC-link with a resistive load (RL), the matrices  $A_2$ ,  $B_2$ ,  $C_2$  and  $D_2$  used for the state-space block are

$$\begin{aligned} A_2 &= \frac{-1}{C(R_L + r_c)}; & B_2 &= \frac{R_L}{C(R_L + r_c)}; \\ C_2 &= \frac{R_L}{R_L + r_c}; & D_2 &= \frac{R_L r_c}{R_L + r_c} \end{aligned} \quad (6)$$

After this mathematical analysis, the student must generate the SIMULINK block of Fig. 2, including the state-space equations of the line filter and the DC-link block. The whole diagram of the VSR with the SPWM controller is presented in Fig. 3. It consists of three PWM signals with duty cycles proportional to the corresponding phase voltage. A predictive controller [10] has been taken to keep the input current in phase with the mains and to regulate DC-link voltage.

Students can easily change the component values and verify what happens to the voltage and current. As an example, Fig. 4 depicts the simulated waveforms of the line voltage, line current and the dc-link voltage, when a step transition from  $I_{out(max)}$  to  $-I_{out(max)}$  is applied to the reference to check the reversible operation of

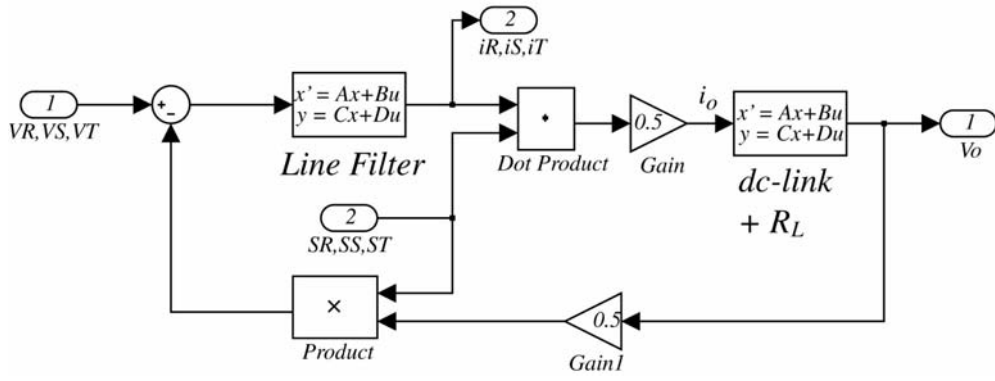


Fig. 2. Block diagram of the VSR in SIMULINK.

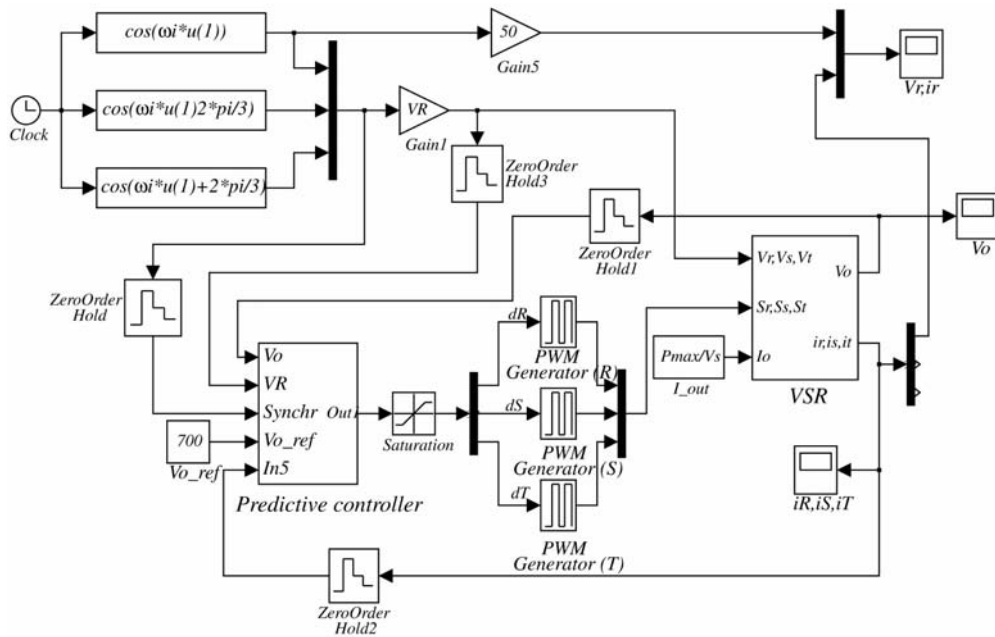


Fig. 3. Block diagram of the VSR with predictive controller in SIMULINK.

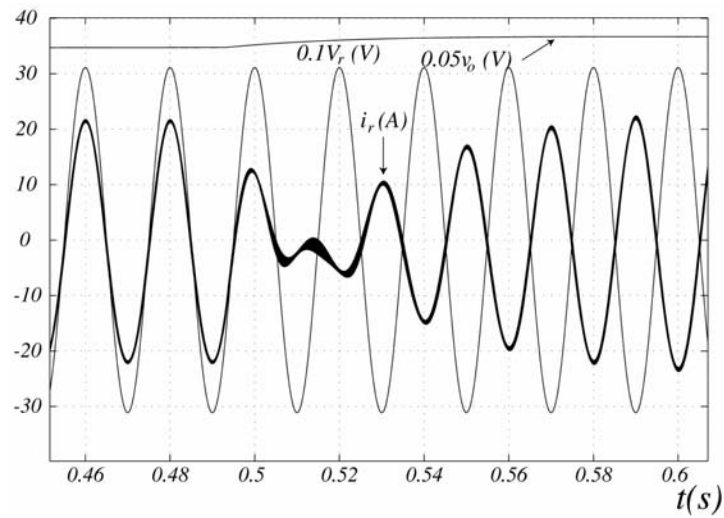


Fig. 4. Simulated waveforms of the line voltage ( $v_r$ ), current ( $i_r$ ) and the dc-link voltage ( $v_o$ ) with a reference step transition from  $I_{out(max)}$  to  $-I_{out(max)}$ .

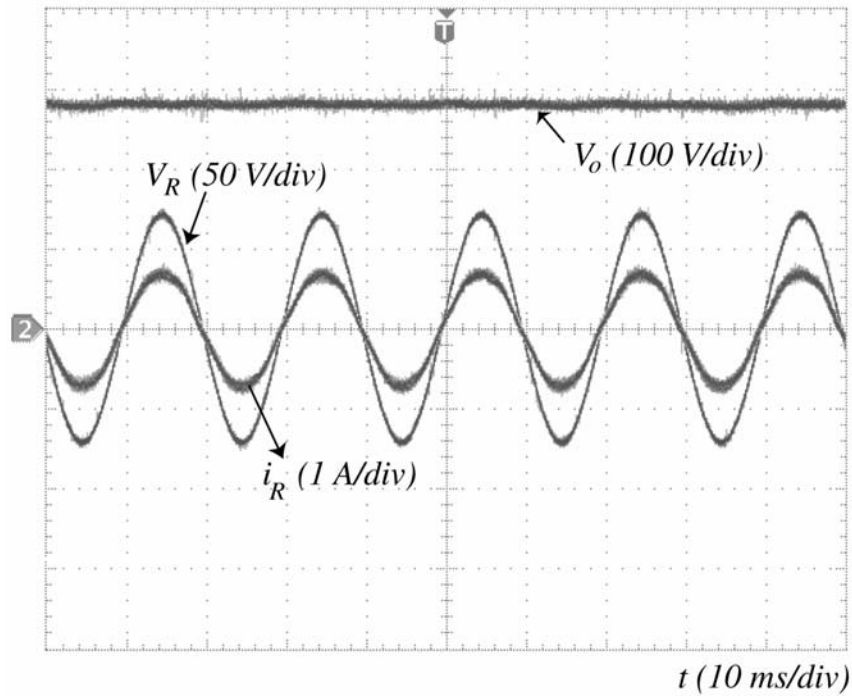


Fig. 5. Experimental waveforms.

the VSR. The values of the parameters used are:  $V_R = 220 V_{rms}$ ,  $L_i = 3.3$  mH,  $r_i = 0.1 \Omega$ ,  $C = 18.8$  mF,  $r_c = 10$  m $\Omega$ ,  $P_{max} = 10$  kW,  $f_s = 20$  kHz. As is shown in Fig. 4, before transition a PFC near to unity is obtained and the DC-link voltage is maintained at 700 V (rectifier mode). After transition the input current is inverted with respect to the input voltage, showing that the current is returned to the mains (inverter mode). In this way, students can verify the reversibility of this topology (the rectifier and inverter operation), by means of a fast simulation in the laboratory that takes about 1 min to simulate an interval of 1 s in a 2.00 GHz Pentium 4, even though this is a closed loop simulation.

With the aim of students being able to see the practical operation of these simulations, we present a prototype that has been developed in our research group. The experimental results of the current and voltage for phase R, along with the output voltage are presented in Fig. 5. Besides showing the practical implementation made, we focus the interest on the effect that real switching commutations produces in the power converter (i.e. the required dead time between commutations).

### MODELLING OF THE CSR

The current source rectifier (CSR) is formed by six voltage-bidirectional and current-unidirectional switches, as shown in Fig. 6. The space vector modulation (SVM) technique will be studied with this converter [2]. The converter to be modelled consists of the line filter (LC), the

power converter and the output filter with inductive load. The line filter and the output filter are modelled by a state-space equation. By applying Kirchoff's laws, the differential equations describing the input filter are

$$\begin{aligned} \dot{i}_j &= -\frac{r_i}{L_i} \cdot i_j + \frac{1}{L_i} \cdot (v_j - v'_j) \\ \dot{v}'_j &= \frac{1}{3C_i(i_j - i'_j)} \quad j = [r, s, t] \end{aligned} \quad (7)$$

We write these equations in a state-space form

$$\begin{aligned} \dot{x} &= A_1 x + B_1 u \\ y &= C_1 x + D_1 u \end{aligned} \quad (8)$$

where  $x = [i_r \ i_s \ i_t \ v'_r \ v'_s \ v'_t]^T$ ,  $u = [v_r \ v_s \ v_t \ i'_r \ i'_s \ i'_t]^T$  and  $y = x$  are the state, the input and the output vectors, respectively. The matrices  $A_1$ ,  $B_1$ ,  $C_1$  and  $D_1$  are

$$A_1 = \begin{bmatrix} \frac{-r_i}{L_i} & 0 & 0 & \frac{-1}{L_i} & 0 & 0 \\ 0 & \frac{-r_i}{L_i} & 0 & 0 & \frac{-1}{L_i} & 0 \\ 0 & 0 & \frac{-r_i}{L_i} & 0 & 0 & \frac{-1}{L_i} \\ \frac{1}{3C_i} & 0 & 0 & 0 & 0 & 0 \\ 0 & \frac{1}{3C_i} & 0 & 0 & 0 & 0 \\ 0 & 0 & \frac{1}{3C_i} & 0 & 0 & 0 \end{bmatrix};$$

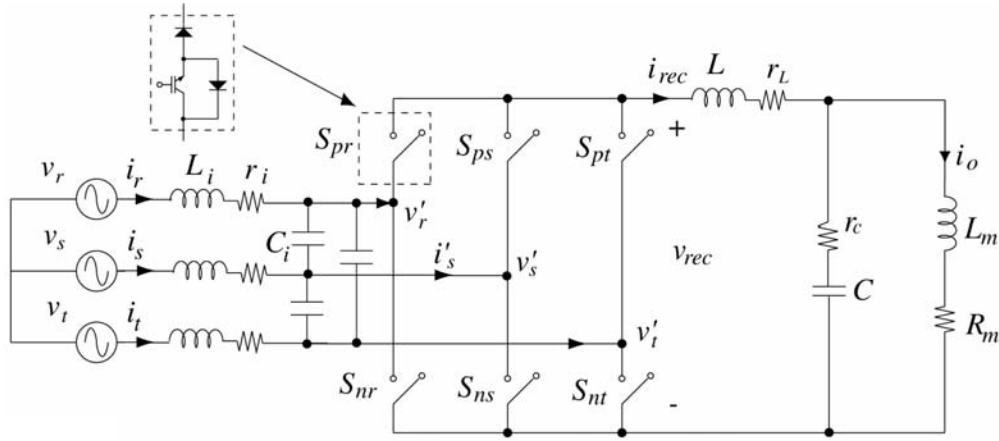


Fig. 6. Three-phase current source rectifier (CSR).

$$B_1 = \begin{bmatrix} \frac{1}{L_i} & 0 & 0 & 0 & 0 & 0 \\ 0 & \frac{1}{L_i} & 0 & 0 & 0 & 0 \\ 0 & 0 & \frac{1}{L_i} & 0 & 0 & 0 \\ 0 & 0 & 0 & \frac{-1}{3C_i} & 0 & 0 \\ 0 & 0 & 0 & 0 & \frac{-1}{3C_i} & 0 \\ 0 & 0 & 0 & 0 & 0 & \frac{-1}{3C_i} \end{bmatrix}$$

$$C_1 = eye(6); \quad D_1 = zeros(6, 6) \quad (9)$$

The non-linear variables that depend on the rectifier switching states are

$$v_{rec} = (S_{pr} - S_{nr}) \cdot v'_r + (S_{ps} - S_{ns}) \cdot v'_s + (S_{pt} - S_{nt}) \cdot v'_t \quad (10)$$

$$i'_j = (S_{pj} - S_{nj}) \cdot i_{rec} \quad j = [r, s, t]$$

where the switching functions  $S_{kj}$  are defined as:

$$S_{kj} = \begin{cases} 1 & ON \\ 0 & OFF \end{cases} \quad k = k = [p, n]; \quad j = [r, s, t].$$

Finally, defining the state, input and output vectors of the output filter as  $x = [i_{rec} \ i_o \ v_c]^T$ ;  $u = [v_{rec}]$ ;  $y = x$  respectively, the  $A_2$ ,  $B_2$ ,  $C_2$  and  $D_2$  matrices yield

$$A_2 = \begin{bmatrix} \frac{-(r_L + r_C)}{L} & \frac{r_C}{L} & \frac{-1}{L} \\ \frac{r_C}{L_m} & \frac{-(r_L + r_C)}{L_m} & \frac{-1}{L_m} \\ \frac{1}{C} & \frac{-1}{C} & 0 \end{bmatrix};$$

$$B_2 = \begin{bmatrix} \frac{1}{L} \\ 0 \\ 0 \end{bmatrix}$$

$$C_2 = eye(3); \quad D_2 = zeros(3, 1) \quad (11)$$

After this explanation, the student must generate the SIMULINK block of Fig. 7, including the

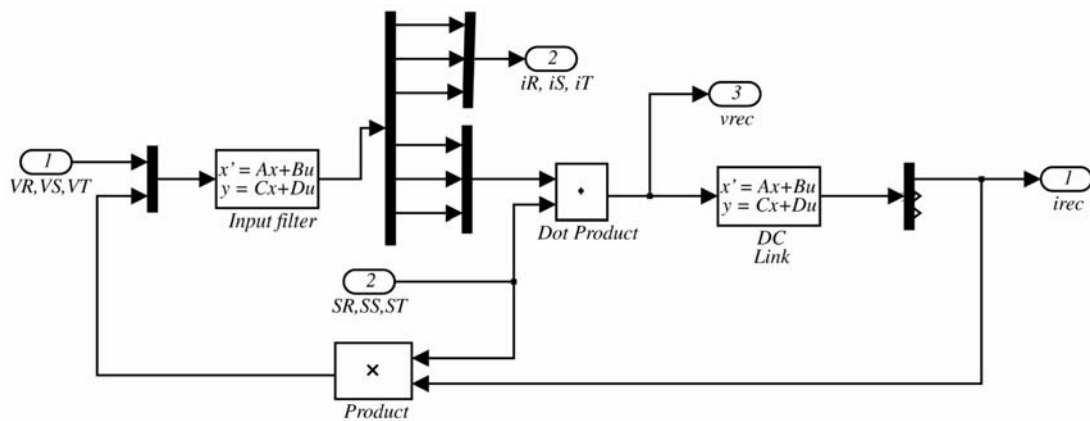


Fig. 7. SIMULINK switching model of the CSR.

state-space equations of the line filter and the output filter with inductive load.

**SVM TECHNIQUE FOR THE CSR**

The SVM technique is widely used in high power three-phase rectifiers [2, 13]. It is based on the representation of the three-phase voltages or currents ( $x_R, x_S, x_T$ ) of a well-balanced system as a time-dependent vector  $X(t)$ , named space vector, in the complex plane, according to the following transformation:

$$X(t) = \frac{2}{3} \cdot (x_R(t) + x_S(t)e^{j(2\pi/3)} + x_T(t)e^{-j(2\pi/3)}) \tag{12}$$

In this course we apply the space vector theory to the CSR of Fig. 6. The CSR has only nine possible combinations of switches, which are represented in the complex plane (Fig. 8) according to the transformation in equation (12), assuming well-balanced currents  $i'_R, i'_S, i'_T$  at the CSR inputs. This gives three zero and six non-zero state-space vectors (SSVs) that divide the plane into six sectors.

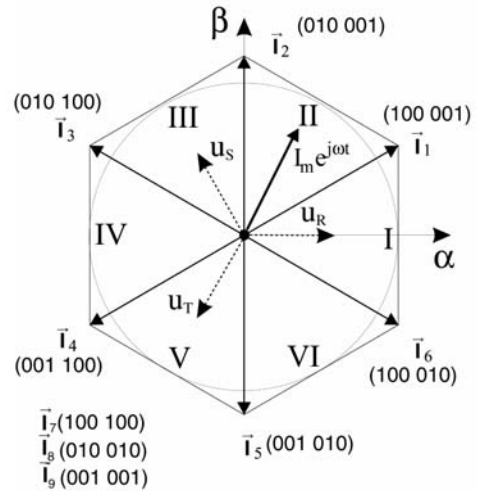


Fig. 8. Switching state vectors in the  $\alpha$ - $\beta$  plane. Numbers in parenthesis indicate ON—'1' or OFF—'0' state for ( $S_{pr}, S_{ps}, S_{pt}, S_{nr}, S_{ns}, S_{nt}$ ).

In the SVM technique, the resulting input current vector  $I(t)$  is synthesised at any given instant by PWM of the two adjacent SSVs and a null vector  $I_n$  ( $I_7, I_8, I_9$ ), as shown in Fig. 8:

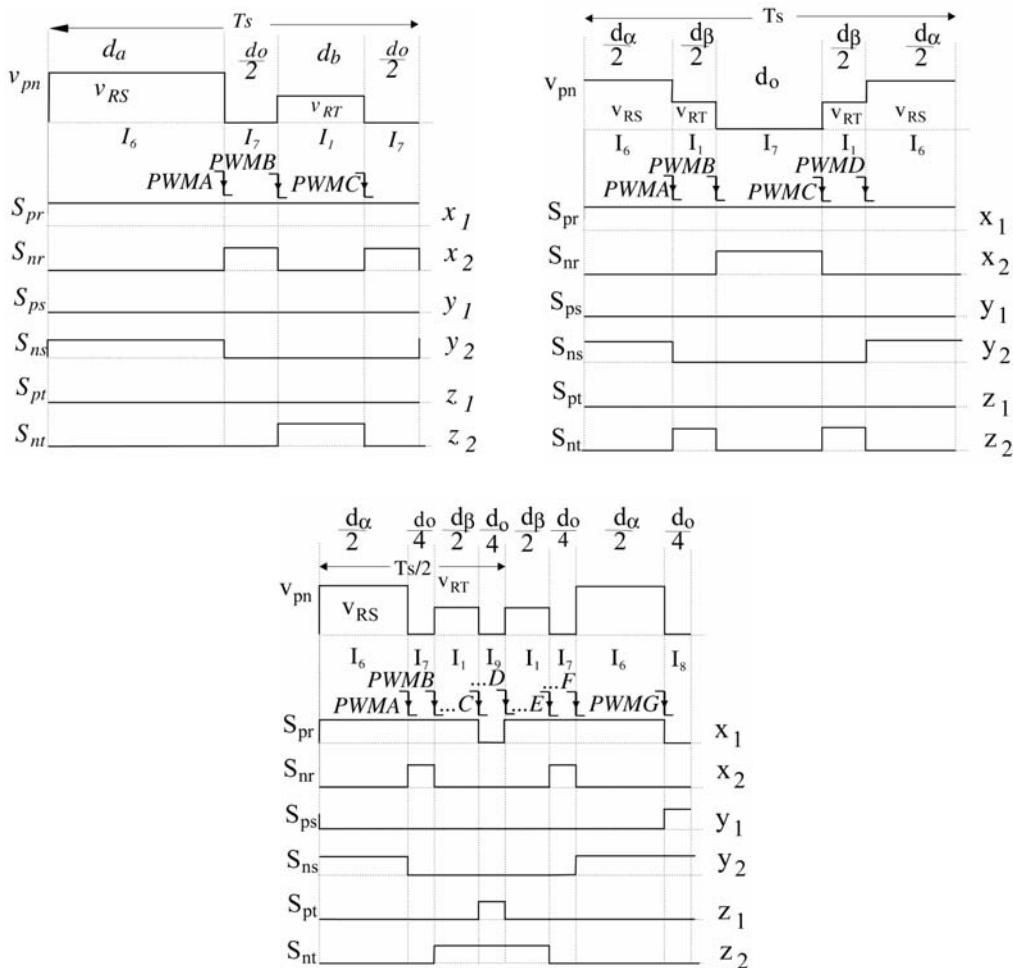


Fig. 9. Three different switching patterns.

Table 1. Distribution of auxiliary signals to transistor gates for each sector

Sector	I	II	III	IV	V	VI
$S_{pr}$	$x_1$	$y_2$	$z_1$	$x_2$	$y_1$	$z_2$
$S_{ps}$	$y_1$	$z_2$	$x_1$	$y_2$	$z_1$	$x_2$
$S_{pt}$	$z_1$	$x_2$	$y_1$	$z_2$	$x_1$	$y_2$
$S_{nr}$	$x_2$	$y_1$	$z_2$	$x_1$	$y_2$	$z_1$
$S_{ns}$	$y_2$	$z_1$	$x_2$	$y_1$	$z_2$	$x_1$
$S_{nt}$	$z_2$	$x_1$	$y_2$	$z_1$	$x_2$	$y_1$

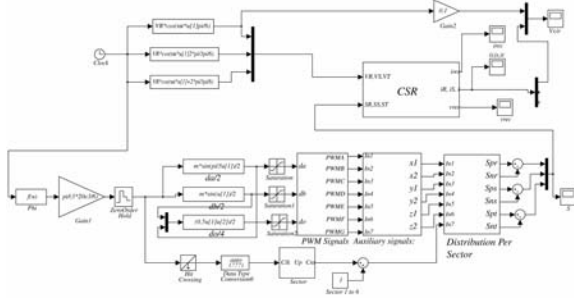


Fig. 10. Simulation model of the CSR with SVM controller in SIMULINK.

$$I(t) = d_\alpha I_\alpha + d_\beta I_\beta + d_o I_n \quad (13)$$

The projections of  $I(I)$  over the SSVs give the following duty cycles:

$$\begin{aligned} d_\alpha &= m \cdot \sin\left(\frac{\pi}{3} - \phi\right) \\ d_\beta &= m \cdot \sin(\phi) \\ d_o &= 1 - d_\alpha - d_\beta \end{aligned} \quad (14)$$

where  $m = |I|/I_L \in [0, 1]$  is named modulation index and  $\phi \in [0, \pi/3]$  is the angle between  $I(t)$  and the lower SSV.

The previous duty cycles indicate the time each SSV has to be applied in the PWM pattern, however the distribution of the adjacent vectors and the null vectors over the period is free [2]. This degree of freedom can be used to improve the harmonic distortion, limit the number of commutations or reduce the output current ripple. Three different switching patterns, shown in Fig. 9, are analysed in the present course. This figure includes the SSVs distribution and the drive-signals  $S_{ij}$  ( $i = p, n$  and  $j = r, s, t$ ) for sector I. These signals can be applied for the remaining sectors by defining six auxiliary signals named  $x_1, x_2, y_1, y_2, z_1, z_2$ , which are distributed differently from the transistor gates according to Table 1.

The SIMULINK diagram of the CSR with the SVM controller is shown in Fig. 10. For implementation of the SVM algorithm, the switching period has been divided in as many PWM signals as the selected profile has transitions, except one. This is implemented in the block diagram of Fig. 10 named ‘PWM Signals’. Duty cycles  $d_\alpha, d_\beta$  and  $d_o$  are calculated by means of Equation (14). Next the

Table 2. Summary of main results

	Profile 1	Profile 2	Profile 3
THD (%)	13.34	3.75	3.01

auxiliary signals are generated as logical combinations of these PWM signals, depending on the selected profile in Fig. 9. The distribution of the auxiliary signals as a function of the present sector is performed with multiplexers, in the block named ‘Distribution Per Sector’ in Fig. 10.

The last implementation is first performed by the teacher for profile of Fig. 9(a). Next, students must modify this schema to simulate the other profiles in Fig. 9, and analyse how these affect the THD of the input current. The knowledge of this procedure for the generation of the PWM signals is extremely useful, because the programming in a digital signal processor can be done following the same philosophy.

Students can also change the component values and verify what happens to the voltages and currents. As an example, values used for simulation are:  $V_R = 110 V_{rms}$ ,  $L_i = 1.3 \text{ mH}$ ,  $r_i = 0.1 \Omega$ ,  $C_i = 1.5 \mu\text{F}$ ,  $L = 1.2 \text{ mH}$ ,  $r_L = 0.1 \Omega$ ,  $C = 200 \mu\text{F}$ ,  $r_c = 50 \text{ m}\Omega$ ,  $L_m = 70 \text{ mH}$ ,  $R_m = 18 \Omega$ ,  $P_{max} = 1.5 \text{ kW}$ ,  $f_s = 20 \text{ kHz}$ . Using the results of a simulation, Fig. 11 shows the input phase current  $i_r$  and phase voltage  $v_r$  for the three selected profiles of Fig. 9, showing that the generated current  $i_r$  is in phase with the corresponding input voltage  $v_r$ , but displays a harmonic distortion that depends on the selected profile. Next, the students must calculate the total harmonic distortion (THD) of the input current  $i_r$  for each one of the selected profiles. Main results are summarized in Table 2.

This analysis shows a better total harmonic distortion for profile 3. The simulation takes about 3 min to simulate an interval of 1 s with a 2.00 GHz Pentium 4, which is fast enough for the classroom.

## CONCLUSIONS

MATLAB/SIMULINK<sup>®</sup> has been successfully used to simulate three-phase PFC rectifiers and their controllers in a power electronics course. This course is not based on circuit simulation alone, since students have to analyse the circuit prior simulation, which improves the understanding of

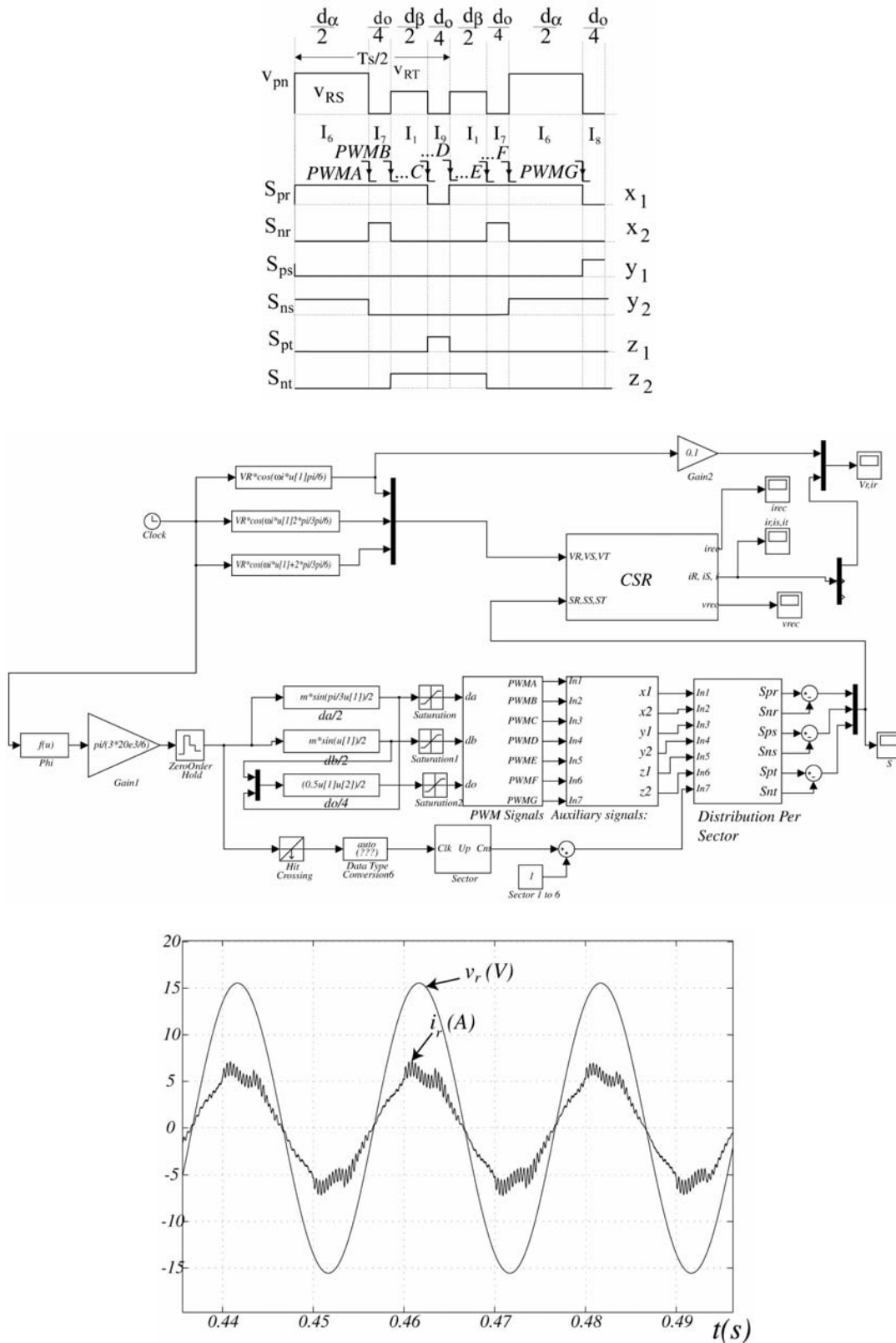


Fig. 11. Simulated current  $i_r$  and phase voltage  $v_r/100$  for the three-different profiles of Fig. 8.



the circuit itself and allows the modelling of the converter. The procedure integrates the teaching of power converter modelling, simulation and analysis of the controller. Two different controllers are analysed in the course: a predictive controller for the VSR and the SVM technique for CSR, showing in both cases a near to unity power factor at the

input. Furthermore, with this procedure the students acquire experience in the analysis, implementation and application of the space vector control in a three-phase PFC rectifier.

*Acknowledgment*—The authors would like to thank the ‘Conselleria d’Empresa, Universitat i Ciència’ of Generalitat Valenciana, Spain, for their financial support (ref.: GV06/164).

## REFERENCES

1. A. de Castro, P. Zumel, O. García, T. Riesgo and J. Uceda, Concurrent and simple digital controller of an AC/DC converter with power factor correction based on FPGA, *IEEE Transactions on Power Electronics*, **18**(3), 2003, pp. 334–343.
2. R. García-Gil, J. M. Espí, E. J. Dede and E. Sanchis-Kilders, A bidirectional and isolated three-phase rectifier with soft-switching operation, *IEEE Transactions on Industrial Electronics*, **52**(3), 2005, pp. 765–773.
3. Berkeley University. SPICE manual. Available online: [bwrc.eecs.berkeley.edu/Classes/IcBook/SPICE](http://bwrc.eecs.berkeley.edu/Classes/IcBook/SPICE)
4. V. F. Pres and J. F. A. Silva, Teaching nonlinear modelling, simulation, and control of electronic power converters using MATLAB/SIMULINK®, *IEEE Transactions on Education*, **45**(3), 2002, pp. 253–261.
5. ANSOFT®, SIMPLORER. Available online: [www.simplorer.com](http://www.simplorer.com)
6. Power Sim Inc., PSIM user manual. Available online: <http://www.powersimtech.com/download.html>
7. MATLAB, The MathWorks Inc., [www.mathworks.com](http://www.mathworks.com)
8. Juing-Huei Su, Chao-Liang Chien, Jiann-Jong Chen and Chien-Ming Wang, Simulink behaviour models for DC–DC switching converter circuits using PWM control ICs, *Int. J. Eng. Ed.*, **22**(2), 2006, pp. 315–322.
9. M. Varadarajan and Simi P. Valsan, MatPECS—A MATLAB-based power electronics circuit simulation package with GUI for effective classroom teaching, *Int. J. Eng. Ed.*, **21**(4), 2005, pp. 606–611.
10. K. Zhou and D. Wang, Digital repetitive controlled three-phase PWM rectifier, *IEEE Transactions on Power Electronics*, **18**(1), 2003, pp. 309–316.
11. D. C. Lee and D. S. Lim, AC voltage and current sensorless control of three-phase PWM rectifiers, *IEEE Transactions on Power Electronics*, **17**(6), 2002, pp. 883–890.
12. N. Mohan, W. Robbins and T. Undeland, *Power Electronics—Converters, Applications, and Design*, John Wiley & Sons, 2<sup>nd</sup> edn, (1995)
13. U. Drofenik and J. W. Kolar, Survey of modern approaches of education in power electronics. *Proceedings of the Third IEEJ/IEEE Joint IAS Power Conversion Conference*, 1, 2002, pp. 305–310.

**R. García-Gil** received his MSc degree in Physics, and the MSc and his Ph.D. degree in Electronic Engineering from the University of Valencia in 1993, 1995 and 2002, respectively. His main research areas are in four-quadrant converters with power factor correction and magnetic component modelling.

**J. M. Espí** received his M.Sc. degree in physics in 1992, with specialization in electronics, and his Ph.D. degree in electrical engineering in 1998, both from the University of Valencia. His research fields are power electronics and control systems.

**J. Castelló** received his BS degree in telecommunications engineering and his MSc degree in electrical engineering from the University of Valencia in 1999 and 2004 respectively. His fields of interest are automatic systems and signal processing.